Steel and Composite Structures, Vol. 10, No. 4 (2010) 361-371
DOI: http://dx.doi.org/10.12989/scs.2010.10.4.361

Effect of FRP composites on buckling capacity of anchored steel tanks

M.A. Al-Kashif[1], H. Ramadan*[1], A. Rashed[2] and M.A. Haroun[3]

[1]*Department of Engineering, Cairo University, Egypt*
[2]*Steel Structures and Bridges, Structural Engineering Department, Cairo University, Egypt*
[3]*Dean of Engineering American University, Cairo, Egypt.*

(Received November 26, 2009, Accepted August 18, 2010)

Abstract. Enhancement in the seismic buckling capacity of steel tanks caused by the addition of fiber reinforced polymers (FRP) retrofit layers attached to the outer walls of the steel tank is investigated. Three-dimensional non-linear finite element modeling is utilized to perform such analysis considering non linear material properties and non-linear large deformation large strain analysis. FRP composites which possess high stiffness and high failure strength are used to reduce the steel hoop stress and consequently improve the tank capacity. A number of tanks with varying dimensions and shell thicknesses are examined using FRP composites added in symmetric layers attached to the outer surface of the steel shell. The FRP shows its effectiveness in carrying part of the hoop stresses along with the steel before steel yielding. Following steel yielding, the FRP restrains the outward bulging of the tank and continues to resist higher hoop stresses. The percentage improvement in the ultimate base moment capacity of the tank due to the addition of more FRP layers is shown to be as high as 60% for some tanks. The percentage of increase in the tank moment capacity is shown to be dependent on the ratio of the shell thickness to the tank radius (t/R). Finally a new methodology has been explained to calculate the location of Elephant foot buckling and consequently the best location of FRP application.

Keywords: steel tanks; seismic design; finite element analysis; elephant's foot buckling; tank shell yielding; fiber reinforced polymers(FRP).

1. Introduction

Fiber reinforced polymer (FRP) composites are increasingly being used in several civil infrastructure applications including use as rebars, bridge decks, strengthening and rehabilitation applications and as new structural systems FRP layers have also a history of successful use in the aerospace, automotive and marine areas. Advanced composites are made up of a polymer matrix reinforced with high-modulus or high-strength fibers. Such composites exhibit linear behavior until failure at very high strains which make them very attractive for the purpose of providing circumferential confinement. The strength properties of FRP depend on the type of fibers, relative fiber content, the type of matrix and the production method. The constituent elements in an FRP composite can combine together to provide the following benefits:

· Provision of more strength and higher modulus of elasticity than most metals.

* Corresponding author, Ph.D., Email: drhazem2003@yahoo.com

- They can be designed to act under tension, flexure, and impact.
- Lighter weight compared to steel, approximately one-fifth that of steel.
- Its ability to be molded to shape several parts of a structure that can be partially or completely prefabricated at the manufacturer's facility and to be installed on site.
- Enhancement of the resistance of the material against creep.
- Its ability to resist different environmental conditions for a prolonged period of time. These environmental exposures include humidity, salt water, alkali solution, freeze/thaw cycles and diesel fuel.

A material testing program was performed by the Aerospace Corporation NASA Design and Manufacturing Guidelines for Aerospace Composites (2000) to assess the durability of the FRP composites. Different parameters were measured to provide an indication of the durability of the material. These parameters include composite panel mass, tensile modulus, strength, failure strain, inter-laminar shear strength, and glass transition temperature. Several research works have been performed using FRP materials to improve the material failure characteristics. Xiao (2004) and Xiao *et al*. (2005) expressed the improvement in buckling resistance of steel tubes filled with concrete in presence of FRP jackets when subjected to axial compression. Teng and Hu (2004) extended the study done by Xiao to investigate the buckling of steel tubes without concrete. Buckling capacity of steel shells subjected to axial compression and internal pressures is also investigated.

Steel tanks are used in several applications including the petroleum industry, municipal water supply systems, and even in nuclear reactors. Failure of tanks would in most cases cause spilling of its contents which could lead to health and environmental hazards. Buckling of steel shells forms one of the main modes of failure in tanks when subjected to seismic excitation. There are two types of buckling usually observed in steel tanks; a) elastic and inelastic buckling in membrane compression inducing the diamond buckling mode and b) elastic-plastic buckling at the shell base resulting in the elephant foot buckling which occurs at higher values of circumferential stresses and causes axi-symmetric bulging of the shell close to ground level. A recent study by Kashef *et al.* (2009) presented a new design criterion to design steel tanks under seismic excitation to resist the elephant foot buckling mode of failure. The occurrence of the elephant foot buckling was seen to coincide with the yielding of the steel shell. Accordingly, the capacity of tanks was defined in terms of the Von-Mises yield stress. It was also shown that Elephant foot buckling is largely influenced by the circumferential stress developed in the tank shell. Therefore, retrofitting of tanks in existence today becomes very important due to its special characteristics. A finite element modeling was performed by Haroun and Bhatia (1999) to study the enhancement of the seismic buckling capacity of liquid-filled shells free at the bottom by the use of FRP retrofit technique. The study was preformed on only one tank with specified dimensions and thickness. The improvement in the buckling capacity of the tank was noted.

The aim of this study is to investigate the enhancement in the elephant foot buckling capacity of steel tanks fixed at its bases caused by the addition of FRP retrofit layers to the outer walls of the tank. The fibers are aligned in one direction to provide high strength characteristics in the direction of the fibers. The advanced composite layers used in this study are made up of Carbon/epoxy and E-glass/polymer systems. Parameters considered through this study are tank radius, tank height, shell thickness and number of carbon layers added to the tanks walls from outside. For each studied tank, one to four carbon/epoxy layers are added to measure the buckling enhancement percentages per each layer. The results are compared to the un-retrofitted tanks and the difference in the stresses and the improvement in the buckling capacity are noted. The deformation and stress distribution in the tanks were also investigated. The use of composite material seemed very appealing in this case to help in reducing the

circumferential stress developed in the tank shell. The suitable location of the FRP layers is finally recommended

2. Finite element model description

A finite element model is created using a general-purpose software Program MARC (1996). Due to symmetry, the tank is modeled as a half cylindrical shell to reduce the solution time. The roof is added to provide stability to the shell near the top of the tank. There is no need to provide a base as the tank is assumed to be fully anchored to the ground through provision of full fixation at shell bottom nodes against movements. The tank is assumed to be filled with water to its full height and the thickness of the steel shell is assumed to be uniform along the tank height with a minimum thickness calculated based on hoop stress developed by the hydrostatic load only with a factor of safety equals two. For minimum thickness estimation, Eq. (1) can be written

$$t = 2\gamma_w HR/\sigma_y \tag{1}$$

Where γ_w is the unit weight of water, R is the tank radius and H is the height measured from the tank base. A 4-noded layered shell element is used to model the walls of steel tank called element no. 75. The steel shell is divided into 5 layers and the FRP layers are further added to the steel layers as the case requires. The FRP composite is modeled as a 2-D orthotropic material with a thickness 0.04 inch for each layer. In unidirectional fiber composites, all the fibers are aligned in one direction to provide high strength characteristics in the direction of the fibers. Since the FRP wrapping are intended to carry load in the circumferential stress, the fibers are oriented to align with the tank circumference. The used model has a sufficient mesh density, and the element dimensions are chosen 30 in × 30 in. To validate the correctness of the results, the mesh size is selected as it yielded deformation values that compared well to the analytical solution of a tank subjected to hydrostatic load only. Also, a number of displacement curves for some tanks issued by Haroun and Bhatia (1999) compared against similarly produced ones by Kashif *et al*. (2009) and it is found that curves confirm pretty well which gives us confidence in the results at hand.

Table 1 shows the parameters considered through this study which are tanks radius R, tank height H, shell thickness t, and number of composite layers added to the tanks walls from outside. For each studied tank, one to four carbon layers are added to measure the buckling enhancement per each added layer. The carbon/epoxy layers are sandwiched between E-glass/polymer layers to prevent direct contact between carbon and steel and to provide symmetry for the FRP layers which is important to avoid layers warping. The E-glass/polymer layer is also used to prevent galvanization action as practical use. An E-glass/polymer layer is firstly added next to the steel shell followed by the carbon

Table 1 List of retrofitted tanks under study

R, inch	H/R	t/R	FRP Layers No.
480	1.0	0.001 & 0.002	One to four
	1.5	0.001 & 0.002	
	2.0	0.002 & 0.0025	
	2.5	0.002 & 0.003	

Table 2 Material properties used through the study

Description	Material	Elastic modulus (Ksi)	Shear modulus (Ksi)	Poisson's ratio	Maximum strength (Ksi)
Fiber direction	Carbon/epoxy Layer	10,000	0.38	0.3	110
Other two directions		0.55	0.38	0.3	
Fiber direction	E-glass/ Polymer Layer	4,000	0.27	0.25	80
Other two directions		0.77	0.27	0.25	
All directions	Steel	30,000	11,628	0.29	36

layers and then another E-glass/polymer glass layer at the end. The FRP layers are applied over the lower part of the tank where elephants foot buckling would normally occur which will be discussed later. Full bonding is assumed between the different layers.

FRP material normally has very high stiffness in the fiber direction and very low stiffness in the other direction. FRP behaves in a linearly elastic form until failure and the properties used in the finite element analysis are listed in Table 2. The steel was assumed to be linearly elastic perfectly plastic and the yield criterion was selected to be Von-Misses.

3. Model loading

Since all tanks are assumed to be filled with water to its full height, they are subjected to both hydrostatic and hydrodynamic loads. Both loading pressure distributions are shown through Fig. 1 for one of the tanks under study. The hydrostatic load varies with height as following

$$P_s = \gamma_w h \tag{2}$$

Where P_s is the hydrostatic pressure, γ_w is the unit weight of water, and h is the height measured from

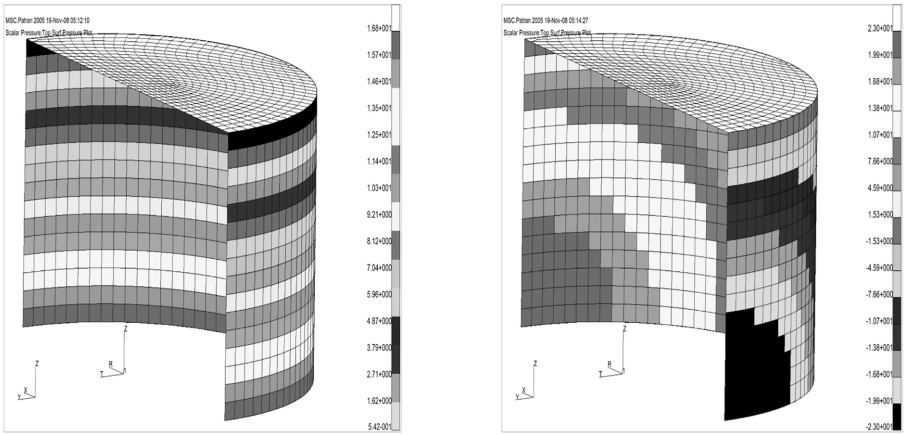

(A) (B)

Fig. 1 Pressure distribution for Tank R = 480 in, H/R = 1 Static and (B) Dynamic

the tank base. The hydrodynamic pressure varies along the height and the circumference of the tank. The hydrodynamic pressure distribution was calculated assuming the following equation

$$P_i = P_0\left[1-\left(\frac{x}{H}\right)^2\right]\cos(\theta) \tag{3}$$

Where x denotes the elevation of a point on the shell measured from the base, H is the liquid depth, θ is the angle measured from the axis of excitation, and P_0 is the pressure amplitude at the tank base at $\theta = 0$. The loads were applied as a uniform surface pressure on the face of each element. The hydrostatic load was firstly applied followed by the hydrodynamic load which was applied in increments until buckling was initiated. The own weight of the tank shell was also taken into consideration.

4. Analysis of results

4.1 Ultimate base moment against displacements

A Displacement curve is drawn for each of the tanks under study in terms of the normalized radial displacement versus a normalized overturning base moment. Figs. 2~5 show the displacement curves for the different tanks with different t/R. The maximum base moment a tank can withstand before it collapses represents the capacity of the tank against seismic, hereinafter referred to as ultimate base moment. The capacity of the tanks is measured in terms of the ultimate base moment. The radial displacement is noted to increase gradually in proportion to the increase in base moment until a point where the radial displacement increases without bound. This point represents the ultimate base moment. It is noticed that the capacity of the tanks is improved in case of provision of more carbon/epoxy layers. Consequently, retrofitted tanks can resist higher base moment. Fig. 6 shows the percentage improvement in ultimate base moment caused by the addition of FRP layers. It is shown that for the same tank dimensions, it can be seen that retrofit works better for lower values of t/R. If the t/R ratio is already high then the improvement caused by the retrofit is less apparent. As the shell thickness used becomes higher than the minimum thickness, the effect of adding FRP layers becomes less. In other words, FRP will not provide remarkable improvement if the steel tank is already over-designed. It is

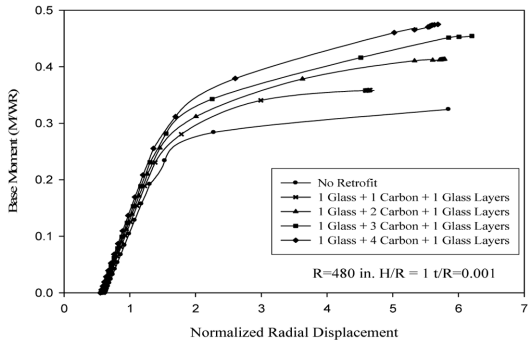

Fig. 2 Displacement curve for tank with H/R = 1, t /R = 0.001, R = 480 in

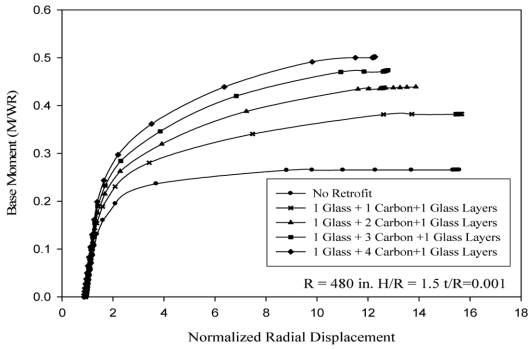

Fig. 3 Displacement curve for tank with H/R = 1.5, t / R = 0.001, R = 480 in

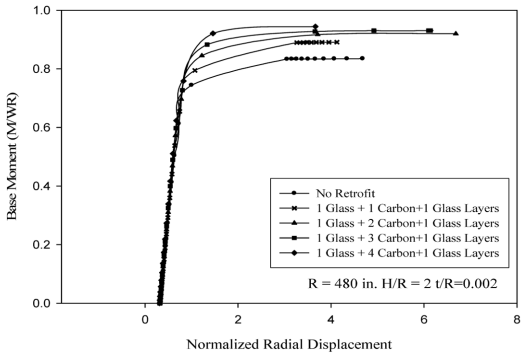

Fig. 4 Displacement curve for tank with H/R = 2.0, t / R = 0.002, R = 480 in

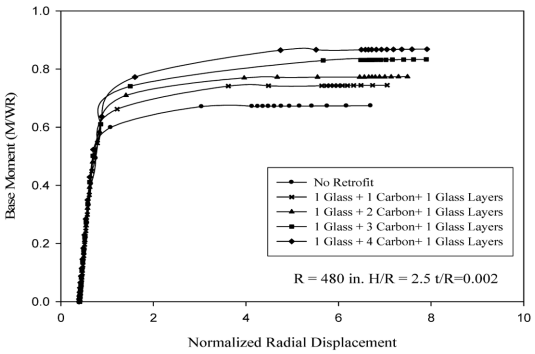

Fig. 5 Displacement curve for tank with H/R = 2.5, t / R = 0.002, R = 480 in

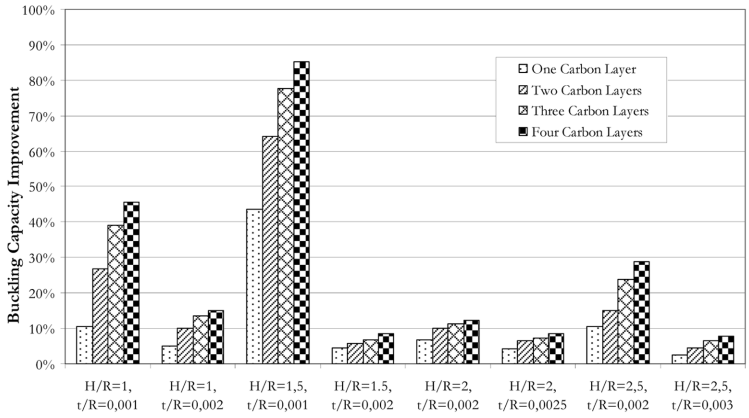

Fig. 6 Percentage increase in ultimate base moments for studied tanks

shown too that the additional improvement in the ultimate buckling capacity diminishes as more Carbon/Epoxy layers are added. Attempting to add more than 4 layers will probably not provide a considerable additional improvement.

4.2 Stresses in steel shell

Stress curves are drawn for some of the tanks under study in terms of the axial, hoop, and Von-Misses as shown in Figs. 7~12. Shell stresses shows that the addition of the FRP layers mainly affects the hoop steel stress which is attributed to the fact that FRP mainly assists in carrying the hoop stress. Since steel has higher stiffness compared to the FRP material, the steel yields way before the FRP reaches failure. After yielding of the steel, the composite starts to carry larger portion of the hoop stress. Therefore, the FRP composite enhances the performance of the tank in two ways. Firstly before yielding of steel, the FRP carries part of the hoop stress thus the steel yields at a higher base moment. Secondly, the composite continues to carry the hoop stress after the yielding of the steel until composite eventually fails. It can also be deduced that the steel tank yields at a higher value of base moment when more carbon layers are added.

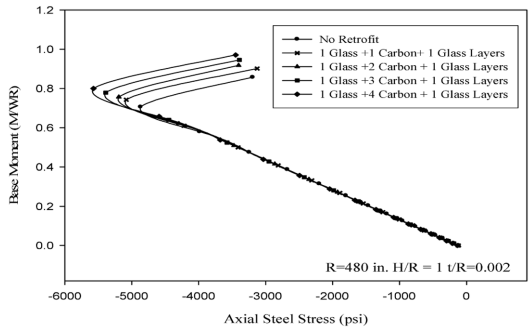

Fig. 7 Axial steel stress for tank with H/R = 1, t / R = 0.002, R = 480 in

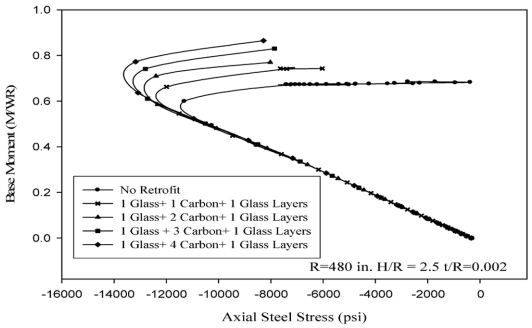

Fig. 8 Axial steel stress for tank with H/R = 2.5, t / R = 0.002, R = 480 in

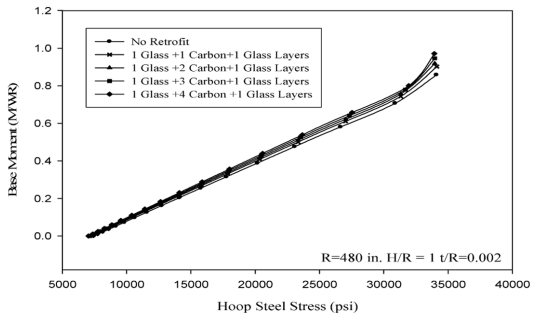

Fig. 9 Hoop steel stress for tank with H/R = 1, t / R = 0.002, R = 480 in

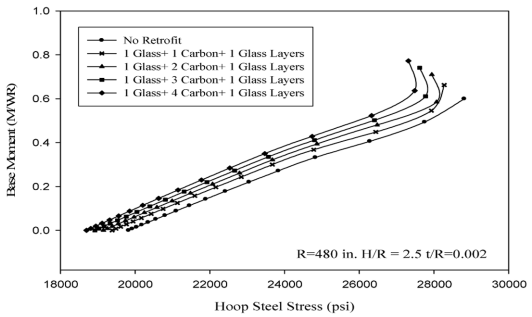

Fig. 10 Hoop steel stress for tank with H/R = 2.5, t / R = 0.002, R = 480 in

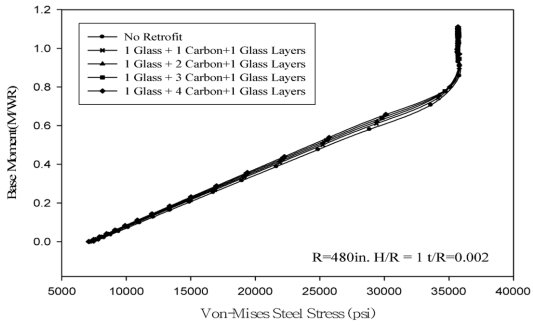

Fig. 11 Von-Misses stress for tank with H/R = 1, t / R = 0.002, R = 480 in

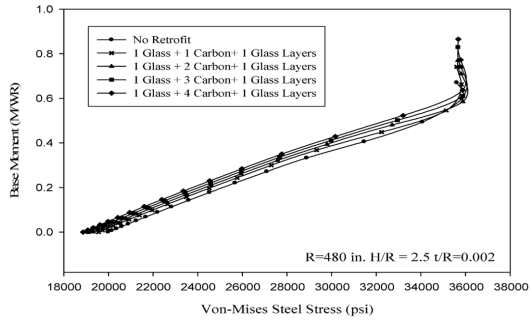

Fig. 12 Von-Misses stress for tank with H/R = 2.5, t / R = 0.002, R = 480 in

4.3 Location of elephant foot buckling above tank base

The differential equation for cylindrical shells is used to solve for the hydrostatic and quasi-static hydrodynamic loads and a distribution of the hoop stress is obtained. The maximum hoop stress occurs at a distance from the base which marks the same area where elephant foot yielding occurs. The deflection of the shell which is related to the load intensity can be expressed by the following differential equation

$$\frac{d^4w}{dx^4} + 4\beta^4 w = \frac{\gamma(H-x) + P_o(1-(x/H)^2)}{Et^3/12(1-u^2)} \tag{4}$$

Where w is the shell deflection at location x from bottom, P_0 is the maximum impulsive pressure at the tank bottom, H is the tank height, t is the tank thickness, γ is Poisson's ratio, E is young's modulus and β is a coefficient defined by

$$\beta^4 = \frac{3(1-v^2)}{R^2t^2} \tag{5}$$

The general solution for the above differential equation can be written in the form

$$w = e^{\beta x}(C_1\cos\beta x + C_2\sin\beta x) + e^{-\beta x}(C_3\cos\beta x + C_4\sin\beta x) - w_p \tag{6}$$

Where w_p represents the particular solution for pressure components. Since the thickness t is very small compared to the radius R and the height H, the shell can be assumed to be infinitely long. Hence C_1 and C_2 are equal to zero. Therefore, the particular solution for the above equation would be

$$w_p = \frac{R^2}{Et}[\gamma(H-x) + P_0(x/H)^2] \tag{7}$$

The first and second terms represent the hydrostatic and the hydrodynamic loads respectively. To solve for the constants C_3 and C_4, the following boundary conditions at the base of tank can be written as follows

$$(w)_{x=0} = 0 \text{ Therefore, } C_3 = \frac{(\gamma H + P_0)R^2}{Et} \tag{8}$$

$$\left(\frac{dw}{dx}\right)_{x=0} = 0 \text{ Therefore, } C_4 = \frac{(\gamma H + P_0 - \gamma/\beta)R^2}{Et} \tag{9}$$

Substituting Eqs. (7)~(9) into 6, one would get

$$w = -\frac{R^2}{Et}[\gamma(H-x) + P_o(1-(x/H)^2) - e^{-\beta x}[(\gamma H + P_o)\cos\beta x + (\gamma H + P_o - \gamma/\beta)\sin\beta x]] \tag{10}$$

Using the following notations,

$$f_1(x) = e^{-\beta x}\cos\beta x \tag{11}$$

$$f_2(x) = e^{-\beta x}\sin\beta x \tag{12}$$

Eq. (10) can be rewritten in the following form

$$w = -\frac{R^2}{Et}[\gamma(H-x) + P_o(1-(x/H)^2) - [(\gamma H + P_o)f_1(x) + (\gamma H + P_o - \gamma/\beta)f_2(x)]] \quad (13)$$

Knowing that the hoop stress N_ϕ can be related to the deflection by

$$N_\phi = \frac{-Ew}{R} \quad (14)$$

Hence, using Eqs. (13), (14), the following equation can be written:

$$N_\phi = \frac{R}{t}[\gamma(H-x) + P_o(1-(x/H)^2) - [(\gamma H + P_o)f_1(x) + (\gamma H + P_o - \gamma/\beta)f_2(x)]] \quad (15)$$

The functions $f_1(x)$ and $f_2(x)$ includes the effect of fixation. These two functions die out rapidly as it is moved away from the fixed end. When the last two terms in the above equation disappear, the hoop stress follows the membrane theory of shells and are equal to

$$N_\phi = \frac{R}{t}[\gamma(H-x) + P_o(1-(x/H)^2)] \quad (16)$$

To determine the location of the maximum hoop stress one needs to equate the derivate of the hoop stress to zero.

$$\frac{dN_\phi}{dx} = \frac{R}{t}\left[(-2\beta(\gamma H + P_0) + \gamma)f_2(x) + \gamma + \frac{2P_0}{H^2\beta}(\beta x)\right] = 0 \quad (17)$$

The location of the maximum hoop stress is further calculated using Eq. (17) for each of the tanks under study and it is found that it fell between 30-60 inches as shown in Table 3. It should be make sure to extend the FRP to cover the region where elephant foot buckling would normally occur. Trying to add more FRP layers, the application height of FRP would have to be increased otherwise possible

Table 3 Estimated location of elephant foot buckling

R, inch	H/R	t/R	β	P_0	x (inch)
480	1	0.001	0.085	16.2	35
	1	0.002	0.06	59.4	50
	1.5	0.001	0.085	7	35
	1.5	0.002	0.06	37	50
	2	0.002	0.06	25.8	50
	2	0.0025	0.054	36	56
	2.5	0.002	0.06	16	50
	2.5	0.003	0.049	37	61

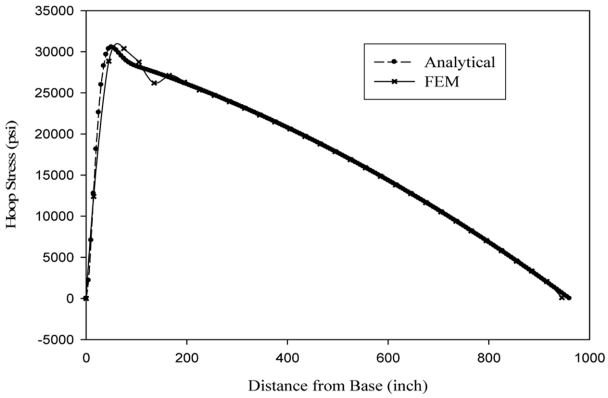

Fig. 13 Distribution of hoop stress for R = 480 in, Tank H/R = 2, t / R = 0.002

buckling of steel above the FRP may be encountered.

Fig. 13 shows the distribution of the hoop stress as determined by equation 17 drawn along with the FEA distribution for a given tank with H/R = 2 and t/R = 0.002. It is shown that the results of the FEA compared very well with the analytical solution obtained in the previous section. In practice, to use the above equation, one would first have to calculate the value of P_0 from Horoun and Housner(1981, 1982) and use this value to estimate the elephant foot buckling location.

5. Conclusion

Based on the results and observations of the present study as related to the tank response under hydrostatic and hydrodynamic loading conditions, the following conclusions can be drawn:

- Moment capacity of steel tanks against elephant foot buckling is improved in case provision of more carbon/epoxy layers.
- For the same tank dimensions, it can be seen that retrofit works better for lower values of t/R. If the t/R ratio is already high then the improvement caused by the retrofit is less apparent.
- Effect of adding FRP layers is very considerable in case of using minimum shell thickness. For thicker shell thickness than the minimum, the improvement caused by the retrofit is less apparent. Therefore, FRP will not provide remarkable improvement if the steel tank is already over-designed.
- A new design methodology is shown to calculate the location of Elephant foot buckling of tanks when subjected to static and hydrodynamic pressures.
- The additional improvement in the ultimate buckling capacity diminishes as more Carbon/Epoxy layers are added. Attempting to add more than 4 layers will probably not provide a considerable additional improvement.

References

American Petroleum Institute-API 650 (2003), "Welded steel tanks for oil storage", Washington D.C.
American Water Works Association-AWWA (2005), "Welded steel tanks for water storage", AWWA-D100, Denver, Colorado.

Haroun, M.A. (1980), "Dynamic analysis of liquid storage tanks", EarthqUake Engineering Research Laboratory, California Institute of Technology, Pasadena, California.
Haroun, M.A. and Al-Kashif, M.A. (2005), "Methodology for design of earthquake resistant steel liquid storage tanks", *Proceeding of the Fifth International Conference on Earthquake Resistant Engineering Structures*, ERES, Skiathos, Greece, May.
Haroun, M.A. and Housner, G.W. (1981), "Seismic design of liquid storage tanks", *J. Tech. Councils-ASCE*, **107**, 191-207.
Haroun, M.A. and Housner, G.W. (1982), "Complications in free vibration analysis of tanks", *J. Eng. Mech*-ASCE, **108**, 801-818.
Haroun, M.A. and Tayel, M.A. (1985), "Response of tanks to vertical seismic excitations", *J. Earthq. Eng. Struct. Dynam.*, **13**(5), 583-595.
Haroun, M.A. and Bhatia, H. (1999), "Enhancement of the seismic buckling capacity of liquid-filled shells", *ASME Publication PVP*, **394**, 185-191.
Housner, G.W. (1963), "The dynamic behaviour of water tanks", *Bull. Seismol. Soc. Am.*, **53**(1), 381-387.
Kashif, M.A., Ramadan, H.M, Rashed, A.A. and M.A. Haroun (2009). "Seismic buckling analysis of steel anchored tanks", *Twelfth International Civil-Comp Conference*, Madrid September, 179-192.
Leon, G.S. and Kausel, E.A.M. (1996), "Seismic analysis of fluid storage tanks", *J. Struct. Eng*-ASCE, **112**(1), 1-18.
Lund, L.V. (1995), "Lifeline utilities lessons, northridge earthquake", *Proceedings of the Fourth U.S. Conference on Lifeline Earthquake Engineering-ASCE*, New York.
Malhorta, P.K., Wenk, T. and Wieland, M. (2000), "Simple procedure for seismic analysis of liquid-storage tanks", *Struct. Eng.*, **10**(3), 197-201.
MARC-Users guide (1996), MARC Analysis Corporation, Palo Alto, California, U.S.A.
NASA Design and Manufacturing Guidelines for Aerospace Composites (2000), Guideline No. GD-ED-2205.
Jaiswal, O.R., Durgesh C.R. and Sudhir K.J. (2007), "Review of seismic codes on liquid-containing tanks", *Earthq. Spectra.*, **32**(1), 239-260.
Malhorta, P.K., Wenk, T. and Wieland, M. (2000), "Simple procedure for seismic analysis of liquid-storage tanks", *Struct.Eng.*, **10** (3), 197-201.
Xiao, Y. (2004), "Application of FRP composites in concrete columns", *Adv. Struct. Eng.*, **7**(4), 335-341.
Xiao, Y. and Choi, K.K. (2005), "Confined concrete-filled tubular columns", *J. Struct. Eng-ASCE*, **131**(3), 488-497.
Teng, J.G. and Hu, Y.M. (2004), "Suppression of local buckling in steel tubes by FRP jacketing", *Proceeding of the second International Conference on FRP composites in civil engineering*, Adelaide, Australia, December.
Teng, J.G. and Rotter, J.M. (2004), *Buckling of thin metal shells*, Spon Press, UK, 42-87.

CC